

Transmission Properties of Doubly Periodic LC Ladder Networks

Ana Flávia G. Greco¹, Joaquim J. Barroso², and José O. Rossi³

Associated Plasma Laboratory

National Institute for Space Research – INPE

12227-010 São José dos Campos, SP, Brazil

¹anaflaviaguedesgreco@gmail.com, ²barroso@plasma.inpe.br, ³rossi@plasma.inpe.br

Abstract—By developing a general formulation described by a system of ordinary differential equations in the time domain, the present work examines filtering and transmission processes that occur in doubly periodic LC transmission lines. The formulation developed herein allows to include an arbitrary number of sections, where even and odd numbered sections are identified by two sets of reactive elements $\{L_2, C_2\}$ and $\{L_1, C_1\}$, respectively. It is shown that lumped-element transmission lines exhibit strong spatial dispersion whereby each line node shows a distinct frequency spectrum. Numerical results by considering inductors and capacitors with typical values of $1\mu\text{H}$ and $1\mu\text{F}$ and driving rectangular pulses of $5\text{-}\mu\text{s}$ width are given and discussed by highlighting the spatial filtering features that occur on such LC lines.

Keywords—doubly periodic transmission lines; lumped-element circuits; spatial dispersion

I. INTRODUCTION

With the continuous increase of operating frequencies of modern high-speed integrated circuits, accurate transmission line models are required to quantify the propagation delay between devices, manage transmission line reflections and crosstalks, besides reducing signal losses. As most electronic devices are time-varying and nonlinear, the analysis of these systems must be performed in the time domain. Analysis in the time domain is also important to predict the transient behavior of power lines excited by external electromagnetic fields produced, for instance, by lightning strokes or by disruptions such as short circuits [1],[2]. In fact, when the system elements are time varying and/or nonlinear, solving the overall network in the frequency domain serves no purpose.

The primary use of transmission lines is to transmit RF power between locations separated by distances comparable to a quarter wavelength. Transmission LC line models include a cascade of distributed elements consisting of series inductances and shunt capacitances with loss resistances and conductances and require a large number of elements and internal nodes to be accurate. When the wires are much shorter than a quarter wavelength, the time lag between the sending and receiving ends will be a small portion of cycle and the system can be analyzed by circuit theory. Expressed in terms

of wavelength, any interconnection of circuit elements that is small compared with the wavelength associated with the highest frequency of interest is called lumped circuit [3]-[5]. As long as this restriction on the size of the circuit holds, the Kirchhoff voltage and current laws are valid, since this restriction reflects the fact that Kirchhoff's laws are approximations of Maxwell's equations.

While the continuous transmission line is described by time-invariant partial differential equations of the hyperbolic type, the lumped circuit equations are ordinary differential equations, which in general are time varying and nonlinear. In light of this, the present work is concerned with the time-domain analysis of lumped transmission LC lines. The configuration of the lines considered here consists of cascade LC cells building up a discrete electrical network of an arbitrary number of unit cells. A system of ordinary differential equations in the time domain is developed in a general formulation where each lumped element in a given section k is assigned with arbitrary, values L_k or C_k . The study is focused on the propagation characteristics of doubly periodic transmission LC lines, where odd-numbered sections has a pair of elements identified by L_1 and C_1 , and even sections have a pair $\{L_2, C_2\}$. In the assignment of the reactive elements, two cases are considered. In the first, the line is composed with elements $L_1C_1 = L_2C_2$, so that the transit time $\delta = \sqrt{LC}$ is the same along every unit cell in the doubly periodic transmission line. In the second case, $L_1/C_1 = L_2/C_2$ for which all the sections have the same characteristic impedance $\sqrt{L/C}$. Various situations are examined by both varying the number of sections and the width of the input rectangular pulse which drives the line.

It is shown that the doubly periodic line exhibits important properties mainly those related with its spatial filtering ability, which constitutes the main contribution of the work as will be discussed in the next sections.

II. CIRCUIT EQUATIONS

A. Periodic LC Transmission Line without Load

Fig.1 shows a generalized LC line without load, where the state variables are the mesh current I_k flowing in the inductor

L_k and the corresponding charge Q_k stored in the capacitor C_k in section k [6]-[8]. It is important from the numerical standpoint that the state variables $\{I_k, Q_k\}$ are taken so that the differential equations are all first order. Losses are also considered by including the inductor resistance $R_{L,k}$, a series resistance $R_{C,k}$ for the capacitor, and the resistance R_s of the voltage source.

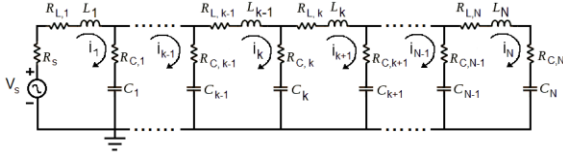


Fig. 1. Unloaded LC ladder network with N sections.

We begin by referring to an unloaded line with only three sections as shown in Fig. 2.

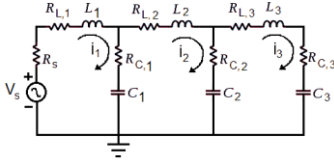


Fig. 2. LC circuit with three sections.

For each section, the Kirchhoff voltage and current laws are applied to the meshes and at the nodes to give

$$\begin{aligned} V_0 - V_1 &= L_1 \frac{dI_1}{dt} + R_{L,1} I_1 \\ V_1 - V_2 &= L_2 \frac{dI_2}{dt} + R_{L,2} I_2 \\ V_2 - V_3 &= L_3 \frac{dI_3}{dt} + R_{L,3} I_3 \end{aligned} \quad (1)$$

where $V_1(t)$, $V_2(t)$ and $V_3(t)$ are the voltages at the nodes and $I_1(t)$, $I_2(t)$ and $I_3(t)$ the mesh currents.

Since

$$\begin{aligned} V_0 &= V_s - R_s I_1 \\ V_1 &= R_{C,1} (I_1 - I_2) + \frac{Q_1 - Q_2}{C_1} \\ V_2 &= R_{C,2} (I_2 - I_3) + \frac{Q_2 - Q_3}{C_2} \\ V_3 &= R_{C,3} I_3 + \frac{Q_3}{C_3} \end{aligned} \quad (2)$$

combining (1) and (2) yields the following system of ordinary differential equations with I_k and Q_k as output variables:

$$\begin{aligned} \frac{dI_1}{dt} &= \frac{V_s}{L_1} - \frac{R_s}{L_1} (I_1) - \frac{R_{L,2}}{L_1} (I_1) - \frac{R_{C,1}}{L_1} (I_1 - I_2) - \frac{Q_1 - Q_2}{L_1 C_1} \\ \frac{dI_2}{dt} &= -\frac{R_{L,2}}{L_2} (I_2) - \frac{R_{C,1}}{L_2} (I_1 - I_2) - \frac{R_{C,2}}{L_2} (I_2 - I_3) + \frac{Q_1 - Q_2}{L_2 C_1} - \frac{Q_2 - Q_3}{L_2 C_2} \end{aligned} \quad (3)$$

$$\begin{aligned} \frac{dI_3}{dt} &= -\frac{R_{L,3}}{L_3} (I_3) - \frac{R_{C,2}}{L_3} (I_2 - I_3) - \frac{R_{C,3}}{L_3} (I_3) + \frac{Q_2 - Q_3}{L_3 C_2} - \frac{Q_3}{L_3 C_3} \\ \frac{dQ_i}{dt} &= I_i, \quad i = 1, 2, 3. \end{aligned}$$

To generalize a system of equations for an arbitrary number of unit cells, separate coupled equations are written for three kinds of sections:

a) Starting section;

$$\begin{aligned} \frac{dI_k}{dt} &= \frac{V_s}{L_k} - \frac{R_s}{L_k} (I_k) - \frac{R_{L,k+1}}{L_k} (I_k) - \frac{R_{C,k}}{L_k} (I_k - I_{k+1}) - \frac{Q_k - Q_{k+1}}{L_k C_k} \\ \frac{dQ_k}{dt} &= I_k \end{aligned} \quad (4)$$

where $k = 1$ and V_s the input voltage, which can be a sinusoidal signal or a pulse of arbitrary shape, either rectangular, triangular or a Gaussian modulated pulse.

b) Intermediate section;

$$\begin{aligned} \frac{dI_k}{dt} &= -\frac{R_{L,k}}{L_k} (I_k) - \frac{R_{C,k-1}}{L_k} (I_{k-1} - I_k) - \frac{R_{C,k}}{L_k} (I_k - I_{k+1}) + \\ &+ \frac{Q_{k-1} - Q_k}{L_k C_{k-1}} - \frac{Q_k - Q_{k+1}}{L_k C_k} \end{aligned} \quad (5)$$

$$\frac{dQ_k}{dt} = I_k; \quad k = 2, 3, \dots, N-1$$

c) Ending section;

$$\begin{aligned} \frac{dI_k}{dt} &= -\frac{R_{L,k}}{L_k} (I_k) - \frac{R_{C,k-1}}{L_k} (I_{k-1} - I_k) - \frac{R_{C,k}}{L_k} (I_k) + \\ &+ \frac{Q_{k-1} - Q_k}{L_k C_{k-1}} - \frac{Q_k}{L_k C_k} \\ \frac{dQ_k}{dt} &= I_k \end{aligned} \quad (6)$$

B. Periodic LC Transmission Line with Load

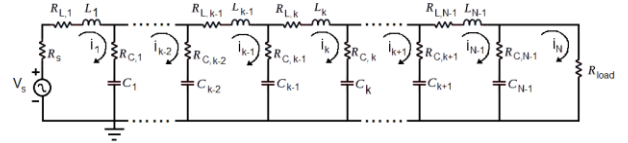


Fig. 3. Loaded LC line with N sections.

A loaded LC line with an arbitrary number of sections is shown in Fig. 3, and analogously to the procedure previously developed we arrive at the following equations:

a) Starting section;

$$\begin{aligned} \frac{dI_k}{dt} &= \frac{V_s}{L_k} - \frac{R_s}{L_k} (I_k) - \frac{R_{L,k+1}}{L_k} (I_k) - \frac{R_{C,k}}{L_k} (I_k - I_{k+1}) - \frac{Q_k - Q_{k+1}}{L_k C_k} \\ \frac{dQ_k}{dt} &= I_k \end{aligned} \quad (7)$$

b) Intermediate section;

$$\begin{aligned} \frac{dI_k}{dt} = & -\frac{R_{L,k}}{L_k}(I_k) - \frac{R_{C,k-1}}{L_k}(I_{k-1} - I_k) - \frac{R_{C,k}}{L_k}(I_k - I_{k+1}) + \\ & + \frac{Q_{k-1} - Q_k}{L_k C_{k-1}} - \frac{Q_k - Q_{k+1}}{L_k C_k} \quad (8) \\ \frac{dQ_k}{dt} = & I_k; \quad k = 2, 3, \dots, N-2 \end{aligned}$$

c) Penultimate section;

$$\begin{aligned} \frac{dI_k}{dt} = & -\frac{R_{L,k}}{L_k}(I_k) - \frac{R_{C,k-1}}{L_k}(I_{k-1} - I_k) - \frac{R_{C,k}}{L_k}(I_k) + \\ & + \frac{Q_{k-1} - Q_k}{L_k C_{k-1}} - \frac{Q_k}{L_k C_k} \quad (9) \\ \frac{dQ_k}{dt} = & I_k; \quad k = N-1 \end{aligned}$$

d) Ending section;

$$\begin{aligned} \frac{dI_k}{dt} = & \frac{R_{C,k-1}}{R_{load} + R_{C,k-1}} \left(-\frac{R_{L,k}}{L_k}(I_k) - \frac{R_{C,k-1}}{L_k}(I_{k-1} - I_k) - \frac{R_{C,k}}{L_k}(I_k) + \right. \\ & \left. + \frac{Q_{k-1} - Q_k}{L_k C_{k-1}} - \frac{Q_k}{L_k C_k} \right) + \frac{I_{k-1} - I_k}{(R_{load} + R_{C,k-1})C_{k-1}} \quad (10) \\ \frac{dQ_k}{dt} = & I_k; \quad k = N \end{aligned}$$

III. RESULTS

In the investigation of frequency response and filtering characteristics of the periodic line, we first look at low-loss ($R_L = R_C = 0.001 \Omega$; $R_s = 0.1 \Omega$) and 10-section line driven by a 1-V amplitude sinusoidal signal. Singly periodic (conventional) LC line is assigned with $L_1 = 1 \mu\text{H}$ and $C_1 = 1 \mu\text{F}$, while the doubly periodic lines are specified for two cases: with $\{L_2 = 2 \mu\text{H}, C_2 = 1/2 \mu\text{F}\}$ or $\{L_2 = 2 \mu\text{H}, C_2 = 2 \mu\text{F}\}$ in the even-numbered sections and with $\{L_1 = 1 \mu\text{H}, C_1 = 1 \mu\text{F}\}$ in the odd sections.

The frequency response of the conventional LC line is illustrated in Fig. 4(a) and, as expected, the line behaves as a low-frequency pass filter, in which the critical frequency is determined by $f_{c1} = 1/\pi\sqrt{L_1 C_1} = 320.0 \text{ kHz}$. The response curve clearly shows the discrete nature of the 10-section line, by noticing ten resonant peaks where the separation between adjacent peaks decreases progressively toward the critical frequency, thus demonstrating that dispersive effects become stronger as f_{c1} is approached. On the far left side of the frequency band ($f < 50 \text{ kHz}$) the oscillations turned out smooth, indicating that the periodic network behaves as a homogenous line.

Analyzing Figs. 4(a)-4(e), it is seen that the frequency response of the doubly periodic line greatly differs from that of the conventional line. We verify the presence of a band gap separating five peaks to the left and five to the right. In the case $L_1 C_1 = L_2 C_2$ [Figs. 4(b) and 4(d)] there appears a new critical frequency $f_{c1}/\sqrt{2} = 226.0 \text{ kHz}$ at the end of the first passband, with the second passband extending up to 340.0 kHz. In the second case where $L_1/C_1 = L_2/C_2$ [Figs. 4(c) and

4(e)] the first passband goes up to $f_{c2}/\sqrt{2} = 113.0 \text{ kHz}$, where $f_{c2} = 1/\pi\sqrt{L_2 C_2}$ with the second one starting at $\sim f_{c1}/\sqrt{2}$. Fig. 4 also demonstrates that the width of the passbands is independent of the characteristic impedance $\sqrt{L/C}$, which has, however, a strong effect on the height of the resonance peaks, as it is clearly apparent in the impedance-mismatched case in Fig. 4(e).

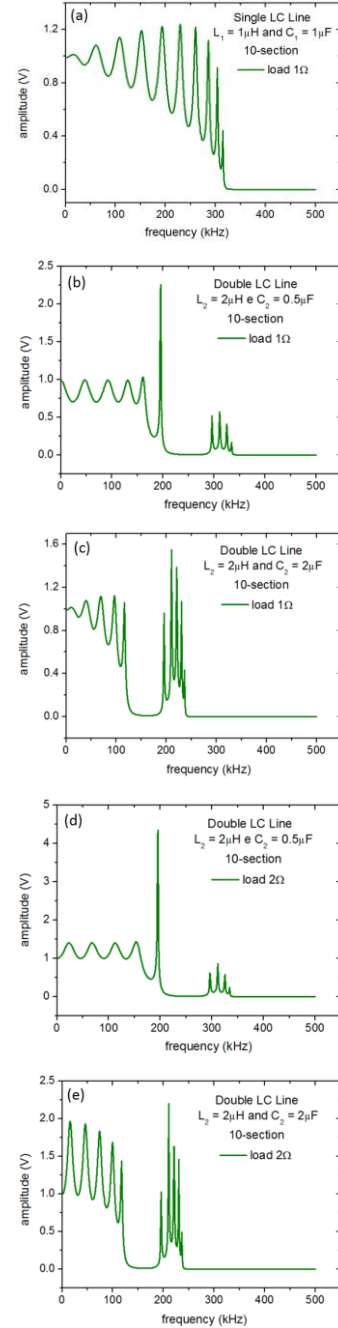


Fig. 4. Signal spectrum at node #10 of LC lines: (a) Singly conventional periodic line with $L_1 = 1 \mu\text{H}$, $C_1 = 1 \mu\text{F}$ and $R_{load} = 1 \Omega$; (b) Doubly periodic line with $L_2 = 2 \mu\text{H}$, $C_2 = 0.5 \mu\text{F}$ and $R_{load} = 1 \Omega$; (c) Doubly periodic with $L_2 = 2 \mu\text{H}$, $C_2 = 2 \mu\text{F}$ and $R_{load} = 1 \Omega$; (d) Doubly periodic with $L_2 = 2 \mu\text{H}$, $C_2 = 0.5 \mu\text{F}$ and $R_{load} = 2 \Omega$; (e) Doubly periodic with $L_2 = 2 \mu\text{H}$, $C_2 = 2 \mu\text{F}$ and $R_{load} = 2 \Omega$.

The transmission and reflection characteristics of the LC networks were investigated by sending through the line a 40- μs -width pulse; the width of 40 μs was selected so that the harmonic content of the input pulse could not be strongly attenuated during its travel along low-loss ($R_L = R_C = 0.001 \Omega$; $R_s = 0.1 \Omega$) and 200-section lines with critical frequencies $\sim 110 \text{ kHz}$.

We first refer to a conventional unloaded line, for which the transit time across each section is $\sqrt{L_1 C_1} = 1 \mu\text{s}$. It is seen in Fig. 5(a) that the reflected pulse returns back to node #2 after a time delay of 400 μs , corresponding to a round-trip time of $2 \times 200 \mu\text{s}$. The distortion on the pulse arises from line mismatching, which is also translated in the frequency spectrum in Fig. 5(b).

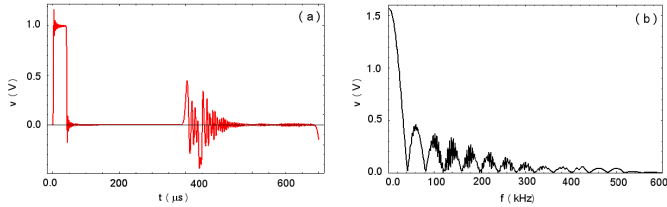


Fig. 5. Signal at node #2 of a singly periodic LC line with $L_1 = 1 \mu\text{H}$, $C_1 = 1 \mu\text{F}$ and $R_{\text{load}} = 1 \Omega$. (a) Transient response and (b) Fourier spectrum.

Figs. 6 and 7 show transmitted and reflected pulses calculated at nodes #100 and #200; the pulse reflected from the load preserves its shape, while the pulse reflected off the sending end emerges with negative amplitude slightly attenuated (third pulse from the left in Fig. 6 and the inverted pulse in Fig. 7). In this example, without resistive load and the line termination being reactive, the reflection coefficient has a unity magnitude, but with a phase shift associated with the reactive ends. In this way, the pulse is completely reflected at the termination of the line with no energy dissipation.

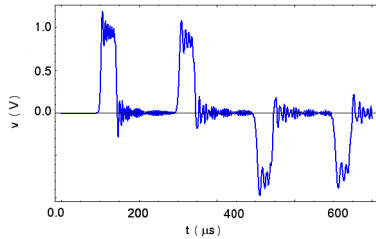


Fig. 6. Transient response at node #100 of a singly periodic LC line with $L_1 = 1 \mu\text{H}$ and $C_1 = 1 \mu\text{F}$.

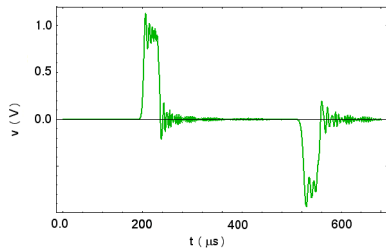


Fig. 7. Transient response at node #200 of a singly periodic LC line with $L_1 = 1 \mu\text{H}$ and $C_1 = 1 \mu\text{F}$.

In the following, looking upon the transmission of the 40- μs pulse along the doubly periodic line with $L_1 C_1 = L_2 C_2$ and loaded with a 1- Ω resistance, we verify in Fig. 8 the occurrence of reflected pulses. Now loading the line with a 2- Ω resistance (the characteristic impedance of a singly periodic line with $L_2 = 2 \mu\text{H}$, $C_2 = 2 \mu\text{F}$), reflections at both ends still persist, as illustrated in Fig. 9, where the reflected pulses have polarity opposite of the corresponding pulses in Fig. 8. But implementing a line, with $L_1/C_1 = L_2/C_2$ terminated with the matching resistance of $1 \Omega = \sqrt{L_2/C_2}$, we see in Fig. 10 that reflections are essentially suppressed in this example; notice also that the transit time for the pulse to reach node #200 increases to 282.0 μs [Fig. 10(b)].

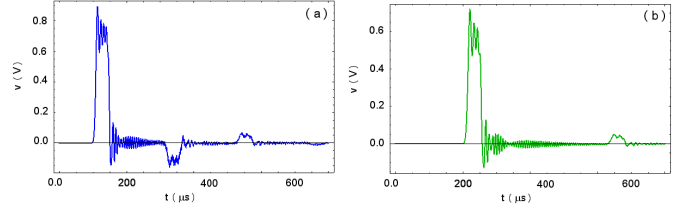


Fig. 8. Rectangular 40- μs pulse transmitted through a doubly periodic LC line with $L_2 = 2 \mu\text{H}$, $C_2 = 0.5 \mu\text{F}$ and $R_{\text{load}} = 1 \Omega$: (a) Transient response at node #100 and (b) transient response at node #200.

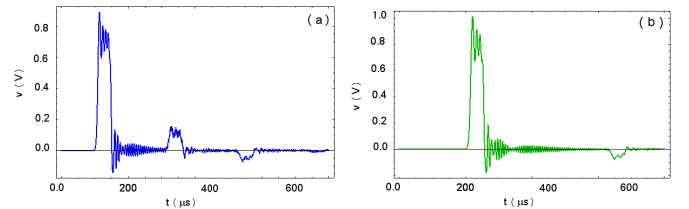


Fig. 9. The same as in Fig. 8 but with $R_{\text{load}} = 2 \Omega$.

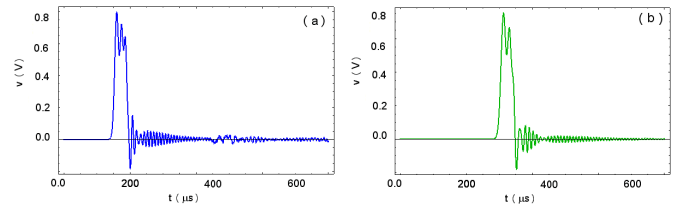


Fig. 10. The same as in Fig. 8 but with $L_2/C_2 = L_1/C_1$ ($L_2 = 2 \mu\text{H}$; $C_2 = 2 \mu\text{F}$).

To investigate the filtering properties of the doubly periodic line, we now consider a 5- μs rectangular pulse such that its Fourier spectrum has multiple sidelobes with width of 200 kHz to encompass the critical frequencies of 320 kHz and 160 kHz as discussed in Fig. 4. Regarding the line with $L_1 C_1 = L_2 C_2$, then we see in Fig. 11 that the spectrum of the transmitted pulse exhibits different features at each node. For example, in Figs. 11(a) and 11(b), corresponding to nodes #2 and #10, there appears in the first sidelobe an isolated passband which is progressively narrowed as the order of the node increases. This phenomenon is interpreted as a local effect at each node, which can be identified as a process that controls the level of filtering. Such a mechanism also manifests itself in the line with $L_1/C_1 = L_2/C_2$ (Fig. 12), but in this case the main lobe is sharply cutoff at 160 kHz.

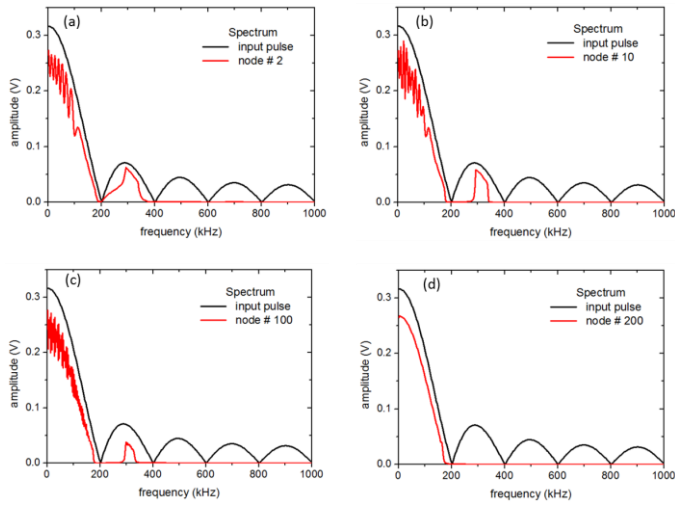


Fig. 11. Spatial filtering in a doubly periodic line with $L_2 = 2 \mu\text{H}$, $C_2 = 0.5 \mu\text{F}$ and $R_{\text{load}} = 1 \Omega$: (a) at node #2, (b) at node #10, (c) at node #100, and (d) at node #200.

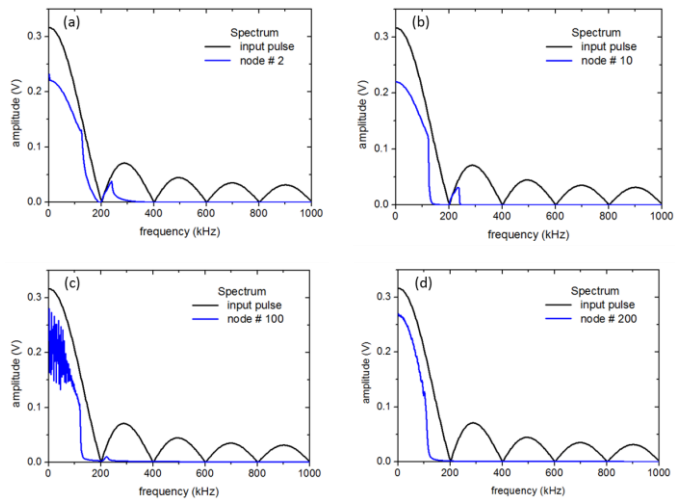


Fig. 12. The same as in Fig. 11, but with $L_2/C_2=L_1/C_1$ ($L_2 = 2 \mu\text{H}$; $C_2 = 2 \mu\text{F}$).

IV. CONCLUSION

A transient and frequency-response analysis of discrete LC transmission lines was performed by formulating a system of generalized circuit equations in the time domain for the lumped elements of an LC ladder network. The system of differential equations was numerically solved with given

initial conditions for the distributions of charge of the capacitors and the currents through the inductors.

In investigating the filtering properties of the doubly periodic LC line driven by a rectangular pulse, it was found that an isolated frequency passband in the Fourier spectrum becomes progressively narrowed toward the end of the line.

In comparison with a singly periodic LC line, this phenomenon arises from the fact that the number of degrees of freedom of the doubly periodic line is doubled, and hence there appear twice as many branches separated by a band gap in the frequency spectrum.

ACKNOWLEDGMENT

Ana Flávia G. Greco thanks the Coordination for the Improvement of Higher Level Personnel (CAPES/Brazil) for their financial support.

REFERENCES

- [1] Tom Dhaene and Daniel De Zutter, "Selection of Lumped Element Models for Coupled Lossy Transmission Lines", *IEEE Trans. Comput. Aid. D.*, vol. 11, no. 7, pp. 805-8015, July, 1992.
- [2] Jyh-Ming Jong, Bozidar Janko, and Vijai Tripathi, "Equivalent Circuit Modeling of Interconnects from Time-Domain Measurements", *IEEE Trans. Compon. Hybr.*, vol. 16, no. 1, pp. 119-126, February 1993.
- [3] M. Remoissenet, *Waves Called Solitons: Concepts and Experiments*. Berlin: Springer, 1999.
- [4] P. C. Magnusson, G. C. Alexander, V. K. Tripathi, and A. Weishaar, *Transmission Lines and Wave Propagation*. New York: CRC Press, 2001.
- [5] C. Caloz and T. Itoh, *Electromagnetic Metamaterials: Transmission Line Theory and Microwave Applications*. New York: Wiley, 2004.
- [6] G.V. Eleftheriades, A.K. Iyer, and P.C. Kremer, "Planar negative refractive index media using periodically L-C loaded transmission lines," *IEEE Trans. Microw. Theory*, vol. 50, pp. 2702-2712, Dec. 2002.
- [7] R. Liu, B. Zhao, X. Q. Lin, and T. J.Cui, "Experimental observation of evanescent-wave amplification and propagation in microwave regime", *Appl. Phys. Lett.*, vol 89, Art. ID 221919, 2006.
- [8] A. F. G. Greco, J. J. Barroso, and J. O. Rossi, "Modeling and Analysis of Ladder-Network Transmission Lines with Capacitive and Inductive Lumped Elements", *J. Electromagnet. Anal. Appl*, vol. 5, pp.213-218, May 2013.